

Revisiting Chebyshev Polynomial and Anisotropic RBF Models for Tabular Regression

Luciano Gerber *¹ and Huw Lloyd^{†1}

¹*Department of Computing and Mathematics, Manchester Metropolitan University,
Dalton Building, Chester Street, Manchester M1 5GD, United Kingdom*

February 27, 2026

Abstract

Smooth-basis models such as Chebyshev polynomial regressors and radial basis function (RBF) networks are well established in numerical analysis. Their continuously differentiable prediction surfaces suit surrogate optimisation, sensitivity analysis, and other settings where the response varies gradually with inputs. Despite these properties, smooth models seldom appear in tabular regression, where tree ensembles dominate. We ask whether they can compete, benchmarking models across 55 regression datasets organised by application domain.

We develop an anisotropic RBF network with data-driven centre placement and gradient-based width optimisation, a ridge-regularised Chebyshev polynomial regressor, and a smooth-tree hybrid (Chebyshev model tree); all three are released as scikit-learn-compatible packages. We benchmark these against tree ensembles, a pre-trained transformer, and standard baselines, evaluating accuracy alongside generalisation behaviour.

The transformer ranks first on accuracy across a majority of datasets, but its GPU dependence, inference latency, and dataset-size limits constrain deployment in the CPU-based settings common across applied science and industry. Among CPU-viable models, smooth models and tree ensembles are statistically tied on accuracy, but the former tend to exhibit tighter generalisation gaps. We recommend routinely including smooth-basis models in the candidate pool, particularly when downstream use benefits from tighter generalisation and gradually varying predictions.

Keywords: tabular regression · Chebyshev polynomials · radial basis functions · generalisation gap · model selection · benchmark

1 Introduction

Practitioners choosing a regression model for tabular data tend to reach for tree ensembles (e.g., random forests, gradient-boosted trees), which have dominated benchmark leaderboards on predictive accuracy [15, 19]. This paper examines whether two smooth-basis models from numerical analysis, Chebyshev polynomial regressors and radial basis function (RBF) networks, can match tree ensembles on predictive accuracy while offering complementary strengths in generalisation, smoothness, and interpretability. Both are well established in function approximation but seldom applied to tabular regression, despite offering practical advantages alongside accuracy. They are directly usable as surrogates in gradient-based optimisation [16, 27],

*L.Gerber@mmu.ac.uk

[†]Now retired.

sensitivity analysis, and other settings where predictions must vary gradually with inputs. Moreover, Chebyshev models yield explicit polynomial coefficients that can be inspected or constrained [43], while RBF models are weighted sums of localised basis functions whose centres and widths carry geometric meaning [8]. These models also train and predict on commodity hardware without GPU acceleration, a practical consideration for the many applied-science and engineering settings where specialised compute is unavailable or uneconomical.

Tabular benchmarks have established a clear picture of predictive accuracy across model families [31, 40], but generalisation gap – the difference between training and test performance – is rarely reported. As an evaluation axis, it can signal excess model capacity and sensitivity to the specific training samples [5], and models that achieve similar held-out scores can differ substantially on it. We argue that generalisation behaviour deserves routine evaluation alongside accuracy, and assess both across diverse application domains.

We revisited these smooth-basis models under contemporary benchmarking standards and with modern optimisation techniques. For RBF networks, we developed an anisotropic formulation (*erbf*) with data-driven centre placement, width initialisation, and gradient-based optimisation of per-dimension widths. These design choices aim to mitigate the instabilities of traditional simultaneous centre-and-width optimisation. For Chebyshev regressors (*chebypoly*), we combined optional pairwise interaction terms with ridge regularisation, synthesising known numerical-analysis building blocks into a practical tool for tabular regression. For settings where the presence of discontinuities is uncertain, we also evaluated a hybrid: Chebyshev model trees (*chebytree*), which use tree splits to identify regime boundaries while fitting Chebyshev polynomials within each leaf. We benchmarked them against established baselines (ridge regression, *ridge*, and a single decision tree, *dt*, representing opposite ends of the bias-variance spectrum), tree ensembles (Random Forest, *rf*, and XGBoost, *xgb*), and a pre-trained tabular foundation model (TabPFN, *tabpfn*) [25]¹ as a representative of the rapidly developing family of transformer-based tabular learners. The comparison spans 55 regression datasets from four domain strata (engineering and simulation; behavioural and social; physics, chemistry, and life sciences; economics and pricing).

Contributions.

1. **Multi-axis benchmark.** We evaluated eight models across 55 datasets on predictive accuracy, generalisation gap, and computational cost. By reporting generalisation gap as a standard evaluation axis – not merely a diagnostic – we show that models that are indistinguishable on accuracy can differ markedly in overfitting behaviour.
2. **Model implementations.** The primary modelling contribution is *erbf*, an anisotropic RBF network with a three-stage training pipeline: data-driven centre placement, width initialisation, and decoupled gradient-based width optimisation in log-space. We also provide a Chebyshev polynomial regressor (*chebypoly*) and a Chebyshev model tree (*chebytree*); these synthesise established numerical-analysis components into practical tabular regression tools. All three are *sklearn*-compatible estimators, available on PyPI (*erbf*, *poly-basis-ml*).

Summary of findings. TabPFN ranks first on accuracy across a majority of datasets but requires GPU inference, is constrained by dataset size, and incurs high prediction latency. Among CPU-viable models, the five competitive models (*xgb*, *rf*, *erbf*, *chebypoly*, *chebytree*) are statistically indistinguishable on accuracy (Friedman test with Nemenyi post-hoc comparison, $\alpha = 0.05$), but smooth models tend to exhibit tighter generalisation gaps, with the smooth model showing the smaller gap in 87% of pairwise comparisons at matched accuracy ($|\Delta R^2| \leq 0.02$). The common default of gradient-boosted trees may not be optimal: we recommend including smooth-basis models in the candidate pool, particularly when generalisation robustness or smooth prediction

¹Our experiments use TabPFN v2.5 weights (*tabpfn* 6.3.1), distributed under a non-commercial licence.

surfaces matter for downstream use.

The remainder of this paper is organised as follows. Section 2 reviews RBF and Chebyshev model families, model trees, and the role of smoothness in generalisation. Section 3 positions the work relative to existing tabular benchmarks and alternative model families. Section 4 describes the model architectures, benchmark design, and evaluation protocol. Section 5 presents results on accuracy, generalisation gap, and computational cost. Section 5.4 develops a practical model selection framework. Section 6 discusses limitations and implications, and Section 7 concludes.

2 Background

2.1 Radial basis function networks

Radial basis function (RBF) networks approximate a target function as a weighted sum of localised kernels centred at selected points in the input space [7, 8]. Centre selection strategies range from random subsets and k -means clustering to greedy procedures that maximise explained variance [11].

Classical RBF networks have seen limited adoption in applied machine learning. Two commonly cited difficulties are that simultaneously optimising centres and widths is non-convex, and that isotropic widths (a single width per basis function) adapt poorly to anisotropic structure in the data [8, 49].

The generalisation from isotropic to anisotropic basis functions has been explored under several names. Zhou et al. [49] provide a comprehensive survey of *hyper basis function* neural networks (HBFNNs), which replace the Euclidean norm with a weighted or Mahalanobis norm, allowing each unit to stretch along different axes. Our *erbf* model adopts diagonal per-dimension widths (a special case of the HBFNN framework) but contributes a decoupled three-stage training pipeline that sidesteps the joint optimisation difficulties described above; the full design is described in section 4.

2.2 Chebyshev polynomials and polynomial regression

Chebyshev polynomials of the first kind form an orthogonal basis on $[-1, 1]$ with numerical properties that make them attractive for regression: the resulting design matrix has far better conditioning than the monomial basis at the same degree, enabling stable fitting of higher-order expansions [43].

Despite this strong theoretical foundation, Chebyshev polynomials have seldom been used as a basis for supervised regression in machine learning. Two well-established alternatives that emphasise smoothness or interpretability are piecewise or additive in structure: MARS [17] fits adaptive hinge-function splines and generalised additive models [22] sum univariate smooth functions. These methods enforce smoothness within each component or segment but not globally across the prediction surface. Our approach combines a Chebyshev expansion with ridge regularisation [24] to provide a globally smooth alternative: the formulation is linear in its parameters once the basis is constructed, so fitting reduces to a single regularised least-squares solve, yielding a smooth, globally defined predictor. The `chebypoly` implementation is described in section 4.

2.3 Model trees

Model trees combine recursive partitioning with local regression models at the leaves. Quinlan [37] introduced M5, which fits linear models in each leaf node; Wang and Witten [46] refined

the approach as M5' with simplified pruning. The appeal of model trees lies in their ability to capture regime changes through the tree structure while modelling smooth relationships within each regime. Our `chebytree` extends this idea by replacing linear leaf models with low-degree Chebyshev polynomial fits (section 4).

2.4 Smoothness and generalisation

Smoothness serves as an implicit regulariser across much of statistical learning. Poggio and Girosi [34] showed that when function approximation is cast as a variational problem penalising derivatives of the fitted surface, the optimal solution takes the form of an RBF or kernel expansion, and ridge regression [24] promotes smoother fits by penalising coefficient magnitude. In a foundational result, Bousquet and Elisseeff [5] formalised the connection between algorithmic stability and generalisation: models with bounded Lipschitz constants (i.e., their output cannot change faster than a fixed rate as inputs vary) produce similar outputs for similar inputs, bounding leave-one-out error. Belkin et al. [4] demonstrated that this classical picture requires revision in the interpolation regime, where over-parameterised models can generalise well despite fitting training data exactly, but for the moderately parameterised models in our benchmark, the stability-generalisation link remains directly applicable.

3 Related Work

Tabular benchmarks and evaluation. Influential large-scale comparisons consistently rank tree ensembles (random forests, 6; gradient-boosted trees, 12) as the strongest general-purpose learners for tabular data [15, 19, 40]. Recent work adds nuance: McElfresh et al. [31] show that neural architectures occasionally surpass boosted trees when hyperparameters are tuned on equal footing, and TabPFN [25] achieves state-of-the-art accuracy on small-to-moderate datasets through a pre-trained transformer. On the methodological side, Demšar [13] established the widely adopted Friedman and Nemenyi tests for multi-classifier comparison, and Cawley and Talbot [10] demonstrated the necessity of nested cross-validation to avoid selection bias. TabArena, the evaluation benchmark introduced alongside TabPFN 2.5 [20], extends this tradition to industry-scale datasets with up to 100 000 training samples, though its evaluation focuses on accuracy rankings. Our benchmark adopts nested cross-validation with Optuna-based inner tuning [2] and reports generalisation gap alongside accuracy, an axis on which model families diverge even when accuracy is matched.

Several recent model families share our interest in smooth, interpretable, or non-tree alternatives for tabular data, each emphasising different trade-offs.

Additive and shape-constrained models. Explainable Boosting Machines [EBMs; 32] fit generalised additive models via boosted shallow trees; Neural Additive Models [NAMs; 1] use per-feature neural networks; Kolmogorov–Arnold Networks [KANs; 30] place learnable spline activations on graph edges. These families prioritise interpretability through additivity, but their structural constraints limit the representation of higher-order multivariate interactions beyond pairwise terms. Our models instead prioritise global smoothness through multivariate basis functions: `chebypoly` constructs explicit cross-product Chebyshev terms that represent higher-order interactions directly, while `erbf`'s multi-dimensional Gaussian kernels couple all input dimensions implicitly through each basis function.

Kernel methods and Gaussian processes. Kernel ridge regression and support vector regression scale as $O(n^3)$ or $O(n^2)$ in time and memory without approximation, making them impractical for many of the datasets in our benchmark. Gaussian processes [38] provide principled

smoothness control through the kernel length-scale and deliver calibrated uncertainty estimates, but suffer the same cubic scaling; inducing-point methods [42] alleviate the cost but introduce additional hyperparameters and approximation error whose impact varies across datasets. Our `erbf` sidesteps this cost structure by fixing K centres ($K \ll n$) and fitting per-centre widths via analytical gradients, yielding $O(nKd)$ complexity with no kernel matrix inversion.

Deep learning for tabular data. FT-Transformer [18], TabNet [3], and NODE [35] adapt attention, gating, and differentiable oblivious decision trees, respectively, to tabular inputs. These architectures can match or exceed tree ensembles on sufficiently large datasets; they occupy a different part of the design space from our models, trading smoothness guarantees and CPU-based training for greater representational flexibility. TabPFN [25] takes a distinct approach: pre-trained on millions of synthetic datasets drawn from a learned prior over data-generating processes, it performs in-context learning at inference time without task-specific training or hyperparameter tuning, achieving strong accuracy on small-to-moderate datasets. We include it in our benchmark as a neural comparator. The field continues to evolve rapidly: tabular foundation models such as TabICL [36] and TabPFN 2.5 [20] now match or exceed tree ensembles on classification benchmarks.

4 Methods

This section describes the three models we contribute to the benchmark: an anisotropic RBF network (`erbf`), a Chebyshev polynomial regressor (`chebypoly`), and a hybrid Chebyshev model tree (`chebytree`). `erbf` and `chebypoly` produce globally smooth (continuously differentiable) prediction surfaces; `chebytree` produces piecewise-smooth surfaces, with smooth polynomial fits within each tree leaf. For each, we outline the mathematical formulation and the algorithmic refinements that make it competitive on tabular regression. Benchmark design and the evaluation protocol are deferred to section 4.5. All three models are implemented in Python, building on NumPy [21], SciPy [45], scikit-learn [33], and joblib [41] for parallelisation. The Chebyshev models are provided by the `poly_basis_ml` package and the RBF network by the `erbf` package; both expose scikit-learn-compatible estimators (`fit/predict` interface) and are available on PyPI (`pip install erbf poly-basis-ml`) and GitHub.²

4.1 Anisotropic RBF Network (`erbf`)

An `erbf`³ places K Gaussian basis functions in the feature space and predicts as a weighted sum of their activations:

$$f(\mathbf{x}) = \sum_{k=1}^K w_k \phi_k(\mathbf{x}) + b, \quad \phi_k(\mathbf{x}) = \exp\left(-\frac{1}{2} \sum_{j=1}^d \frac{(x_j - c_{kj})^2}{\sigma_{kj}^2}\right), \quad (1)$$

where $\mathbf{c}_k \in \mathbb{R}^d$ is the centre, $\boldsymbol{\sigma}_k \in \mathbb{R}_{>0}^d$ is the width vector, w_k is the output weight, and b is a bias. The key distinction from isotropic RBF networks is that each basis function has a separate width along each feature dimension ($K \times d$ width parameters in total), allowing anisotropic adaptation to local data structure.

Classical RBF training optimised centres and widths simultaneously, typically via gradient descent or metaheuristics, creating a high-dimensional non-convex problem prone to poor local minima. These training difficulties, together with the limited expressiveness of isotropic

²<https://github.com/gerber1/erbf> and <https://github.com/gerber1/poly-basis-ml>

³The “e” in `erbf` stands for *ellipsoidal*: each basis function’s iso-activation contour forms an axis-aligned ellipsoid when widths differ across dimensions.

widths, contributed to RBF networks falling out of mainstream use. The pipeline described below is designed to mitigate both issues: centres are fixed before width optimisation begins, and anisotropic widths adapt to per-feature relevance.

The conceptual insight motivating this decomposition is that centre placement and width adaptation serve distinct purposes: centres determine *where* the model allocates representational capacity, while widths determine *how* that capacity responds to local data structure. Conflating these in a single optimisation loop (the classical approach) couples two sources of non-convexity: the loss surface contains both the combinatorial difficulty of choosing good locations and the continuous difficulty of shaping the basis functions around them. Lipschitz-guided centre placement addresses the first problem by exploiting target variation directly: regions where the function changes rapidly need finer coverage, so sampling probability proportional to local Lipschitz estimates concentrates centres where they matter most, without requiring gradient-based search over discrete placements. With centres fixed, width optimisation becomes a continuous problem in $\mathbb{R}^{K \times d}$ that L-BFGS-B [9] can solve efficiently via analytical gradients. The decoupling also mitigates a plausible failure mode of joint optimisation: the optimiser may drive widths toward zero around poorly placed centres to fit local noise, producing sharp peaks that overfit. Fixing centres first constrains width optimisation to refine a geometrically sensible initial configuration rather than compensate for bad placement.

Training proceeds in three decoupled stages.

Stage 1: Centre placement. Two strategies are available. The default, Lipschitz-guided placement (`center_init='lipschitz'`), is supervised: we estimate the local Lipschitz constant at each training point as

$$L_i = \max_{j \in \text{kNN}(i)} \frac{|y_i - y_j|}{\|\mathbf{x}_i - \mathbf{x}_j\| + \epsilon}, \quad (2)$$

using five nearest neighbours, where ϵ is a small constant for numerical stability; extreme values are clipped at the 99th percentile for robustness. The K centres are then sampled without replacement from the training set, with selection probability proportional to L_i . This concentrates centres in high-gradient regions where the target function changes rapidly, allocating modelling capacity where it is most needed. The alternative, K -means clustering (`center_init='kmeans'`), is unsupervised and distributes centres according to feature-space density without accounting for target variation.

Stage 2: Width initialisation. Good width initialisation substantially reduces the burden on subsequent optimisation. The `width_init` parameter selects between two methods:

Local ridge (`width_init='local_ridge'`, supervised): for each centre \mathbf{c}_k , a ridge regression is fitted to its k nearest training points ($k = \min(100, \lfloor n/K \rfloor)$, floored at 10), yielding per-feature coefficients β_j . The initial width is set as $\sigma_{kj} = \tau \sqrt{\text{Var}(x_j) / |\beta_j|}$, where $\text{Var}(x_j)$ is the variance of feature j among the centre's neighbours and $\tau = 1.5\sqrt{d}$ is a dimensional scaling factor (same rationale as for local variance below), so that features with strong local predictive power (large $|\beta_j|$) receive narrow widths (high sensitivity) while locally irrelevant features receive wide widths (smoothing). *Local variance* (`width_init='local_variance'`, unsupervised): widths are set proportional to the local standard deviation of each feature among the centre's neighbours, scaled by \sqrt{d} so that the Gaussian activation remains approximately $e^{-1/2}$ at the typical neighbour distance regardless of dimensionality (the exponent sums d squared terms, so per-dimension widths must grow with \sqrt{d} to compensate). This purely geometric initialisation ignores target values and is appropriate when features contribute roughly equally.

Stage 3: Width optimisation. With centres fixed, widths are optimised by minimising the mean squared error via L-BFGS-B, operating in log-space ($\theta_{kj} = \log \sigma_{kj}$) to enforce positivity.

Log-space parameterisation also provides implicit regularisation: the multiplicative update structure prevents individual widths from collapsing to zero, and the loss landscape is more uniform across scales, so that a width change from 0.01 to 0.02 receives the same gradient magnitude as a change from 1.0 to 2.0. Analytical gradients are computed in $O(n \cdot K \cdot d)$ per iteration; the activation kernel is JIT-compiled via Numba [28] for efficiency.

Output weights. Given the activation matrix $\Phi \in \mathbb{R}^{n \times K}$, the output weights are obtained by ridge regression: $\mathbf{w} = (\Phi^\top \Phi + \alpha \mathbf{I}_K)^{-1} \Phi^\top \mathbf{y}$, where \mathbf{I}_K is the $K \times K$ identity matrix.

Automatic scaling of K . Setting `n_rbf='auto'` applies the empirical heuristic

$$K = \text{clip}(\max(40, 2d), 20, \min(200, n/10)),$$

scaling roughly with dimensionality while respecting sample-size and computational constraints.

Hyperparameters. The model exposes four hyperparameters: the number of centres `n_rbf` (which can be set to `auto` for adaptive scaling as described above, or fixed); the ridge penalty `alpha` for the output weights; the centre placement strategy `center_init` (Lipschitz-guided or K -means); and the width initialisation method `width_init` (local ridge or local variance).

Training summary. Algorithm 1 in the appendix summarises the three-stage pipeline.

4.2 Chebyshev Polynomial Regressor (`chebypoly`)

The Chebyshev polynomial regressor expands each input feature into a univariate polynomial basis and fits a linear model in the expanded feature space. We use Chebyshev polynomials of the first kind, T_n , defined by the three-term recurrence

$$T_0(x) = 1, \quad T_1(x) = x, \quad T_{n+1}(x) = 2x T_n(x) - T_{n-1}(x), \quad (3)$$

which form an orthogonal basis on $[-1, 1]$. Standard monomial bases $(1, x, x^2, \dots)$ suffer from severe ill-conditioning at moderate degrees, whereas Chebyshev polynomials remain well-conditioned and achieve near-minimax approximation error [43].

Feature expansion. Given d input features and a maximum degree c (the complexity parameter), we construct a design matrix whose columns are the Chebyshev evaluations

$$T_0(x_1), T_1(x_1), \dots, T_c(x_1), T_1(x_2), \dots, T_c(x_d),$$

yielding $1 + d \cdot c$ basis terms (the constant T_0 is included only for the first feature to avoid redundant intercepts). The Vandermonde matrix is constructed using `numpy.polynomial.chebyshev`. Inputs are first mapped to $[-1, 1]$ using a min-max scaler, and values outside the training range are clipped (`clip_input`) for numerical stability.

Interaction terms. Univariate Chebyshev terms capture per-feature nonlinearity but miss bivariate relationships. When `include_interactions` is enabled, we augment the basis with pairwise product interactions $x_i \cdot x_j$ between scaled features, adding up to $d(d-1)/2$ terms. These are products of the original scaled features, not of polynomial evaluations; cross-polynomial terms such as $T_2(x_i) \cdot T_3(x_j)$ would produce a combinatorial explosion. To limit basis size when dimensionality is high ($d > 30$) we restrict interaction pairs to the top half of features ranked by variance. When `max_interaction_complexity = 2`, each product term is further expanded by appending its Chebyshev evaluation $T_2(x_i \cdot x_j)$; at the default value of 1, only the raw products are used.

Regularisation and prediction. The expanded design matrix is solved by ridge regression. We tested elastic net regularisation [50] but found that coordinate descent at low α values incurs substantial computational overhead without improving accuracy; ridge proved sufficient. Predictions are clipped to $\pm 3\sigma$ of the training target to suppress extrapolation artefacts.

Hyperparameters. Two hyperparameters govern the core basis expansion: the polynomial degree (complexity), which sets the expressiveness of the univariate basis, and the ridge penalty (alpha). Two further parameters control interaction terms: whether to generate pairwise product features (include_interactions), and the degree to which those terms are expanded (max_interaction_complexity).

4.3 Chebyshev Model Tree (chebytree)

The Chebyshev model tree is a piecewise-smooth hybrid: a decision tree partitions the feature space into axis-aligned regions, and each leaf fits an independent Chebyshev polynomial regressor. This combines the tree’s capacity for detecting regime boundaries (thresholds, interaction effects, discontinuities) with the smooth local fits provided by Chebyshev polynomials.

Architecture. A decision tree regressor is grown with tunable max_depth and min_samples_leaf. At prediction time, each sample is routed to its leaf by the tree structure, and the leaf-local Chebyshev polynomial generates the prediction. Leaves with insufficient samples fall back to the tree’s own constant prediction to avoid overfitting degenerate local fits. Each leaf model is fitted independently using ridge regression on the Chebyshev-expanded features of the leaf’s training subset.

Recommended Usage. Because each leaf contains only a subset of the training data, leaf polynomials should generally use a lower degree than a global Chebyshev fit to avoid overfitting. Interaction terms are omitted from leaf models both to reduce overfitting risk and to keep the per-leaf basis size tractable. The min_samples_leaf parameter can be expressed as a fraction of the training set, ensuring leaves remain large enough for stable polynomial fits.

Hyperparameters. The model exposes four hyperparameters: the per-leaf polynomial degree complexity; the tree depth max_depth; the minimum leaf fraction min_samples_leaf; and the ridge penalty alpha. At the extremes of this space, a shallow tree with low-degree polynomials yields a simple piecewise-linear model, while a deep tree with high-degree polynomials produces many nonlinear local surfaces.

4.4 Datasets

We assembled 55 regression datasets from seven sources: OpenML [44], UCI [14], PMLB [39], MoleculeNet [48], Hugging Face Datasets, scikit-learn generators, and custom synthetic functions. Dataset sizes range from $n = 442$ to 581,835 and dimensionality from $d = 2$ to 1,024; table 5 in the appendix provides the full list with metadata.

Stratification. We grouped the datasets into four strata by application domain, as an exploratory lens for examining whether model performance varies with the type of problem. The assignments reflect our judgement about which domains are more likely to produce smooth target functions, or to involve thresholds or discrete structure; they are not a validated classification and individual datasets may not conform to the stratum-level expectation.

S1: Engineering/Simulation (13 datasets). Systems typically governed by physical laws or smooth equations. Representative datasets include airfoil_noise, power_plant, friedman1, and Feynman physics problems.

S2: Behavioural/Social (10 datasets). Human decision-making, preferences, and demand, often involving implicit thresholds (ratings, satisfaction scores, usage counts). Six datasets have discrete targets (e.g., integer-valued ratings or scores treated as continuous regression). Representative datasets include `wine_quality`, `Bike_Sharing_Demand`, and `student_performance`.

S3: Physics/Chemistry/Life Sciences (16 datasets). Natural-science measurements – likely often smooth, but may contain phase transitions or abrupt property changes. Three molecular datasets (`esol`, `freesolv`, `lipophilicity`) are distributed as SMILES strings (see preprocessing below). Representative datasets include `superconduct`, `esol`, `lipophilicity`, and `diabetes`.

S4: Economics/Pricing (16 datasets). Pricing, insurance, and real estate – domains that often involve explicit rules, tax brackets, and policy thresholds. Representative datasets include `california_housing`, `diamonds`, `house_sales`, and `medical_charges`.

4.5 Benchmark Design and Evaluation Protocol

We applied the evaluation protocol detailed below for 8 regression models on the 55 datasets described in section 4.4. The models span five groups: two smooth-basis models (`chebypoly`, `erbf`); a smooth-tree hybrid (`chebytree`); two tree ensembles (`rf`, `xgb`); a pre-trained tabular transformer (`tabPFN`); and two baselines at opposite ends of the bias-variance spectrum, linear ridge regression (`ridge`) and decision tree (`dt`).

Preprocessing pipeline. All models receive identically preprocessed data. The pipeline has two stages: dataset-level steps applied once before cross-validation splitting, and fold-level steps applied within each CV fold.

Dataset-level preprocessing.

1. *Feature engineering* (dataset-specific). Three molecular datasets distributed as SMILES strings are converted to 16 standard RDKit [29] physicochemical descriptors.
2. *Quality filtering* (all datasets, unconditional). Features with more than 50% missing values are dropped, as are quasi-constant features (mode frequency >95%).
3. *Sample reduction*. Datasets exceeding $n = 50,000$ are subsampled without replacement, keeping tuning tractable and satisfying the input constraints of `tabPFN`.
4. *Feature prefiltering*. For datasets with $d \geq 25$: features with $|\rho_{\text{Spearman}}| < 0.05$ are removed except those rescued by MI (features in the bottom 30% by Spearman rank but in the top 30% by MI are retained), preserving non-monotonic relationships that a linear correlation filter would discard.
5. *Dimensionality reduction*. If $d > 50$ after prefiltering, the top- k features are selected by mutual information to keep computational costs tractable.

Because these steps are applied before splitting, the feature-selection ranking involves mild test information leakage. We accepted this to ensure identical feature sets across all models and folds; the resulting bias is shared equally rather than favouring any particular family.

Nested cross-validation. Evaluation follows a nested cross-validation (CV) design to obtain unbiased estimates of generalisation performance while tuning hyperparameters.

- *Outer loop*: 5-fold CV provides held-out test folds for final evaluation.
- *Inner loop*: within each outer training set, hyperparameter search takes place with an adaptive number of inner folds (3-fold CV when $n \geq 1,000$, 5-fold otherwise). The model is then refit on the full outer training set using the best configuration before evaluation on the held-out outer test fold.

For models that support early termination (here, XGBoost), 15% of the outer training set is held out as a validation set for early stopping.

Fold-level preprocessing. The following data transformations are fitted on training data and applied to both training and validation/test splits within each CV fold.

- *Imputation.* Median for numeric features, mode for categorical features.
- *Categorical encoding.* Categorical features are converted to numeric via target encoding (TargetEncoder with smooth='auto' via sklearn).
- *Standardisation* (model-dependent). `ridge` and `tabPFN` receive standardised features; tree-based models do not; Chebyshev and `erbf` models apply internal scaling.

Hyperparameter tuning. Hyperparameters are optimised with Optuna [2] using the TPE sampler (multivariate=True) and a MedianPruner for early termination of unpromising trials ($n_{\text{startup}} = 3$, $n_{\text{warmup}} = 1$). Trial budgets are roughly proportional to search-space dimensionality: `ridge` 20, `dt` 25, `rf` 25, `xgb` 50, `erbf` 30, `chebypoly` 30, `chebytree` 30; `tabPFN` uses no tuning (zero-shot). Search spaces use log-uniform distributions for regularisation parameters, integer ranges for structural parameters (e.g., tree depth, number of centres), and categorical choices for algorithmic variants (e.g., centre placement, width initialisation). Full per-model search-space definitions are provided in section B.

Evaluation metrics. We report adjusted R^2 (hereafter \bar{R}^2) as the primary accuracy metric and the generalisation gap, defined as training minus validation R^2 , as a measure of overfitting. For all models, predictions are clipped to $[y_{\min} - 3\sigma, y_{\max} + 3\sigma]$ (computed from the training fold targets) to prevent catastrophic extrapolation from inflating error metrics. Each metric is aggregated as both mean \pm standard deviation and median across the five outer folds.

Ranking and statistical testing. Models are ranked per-dataset by \bar{R}^2 ; models that could not run on a dataset receive worst rank (k , the number of models in the comparison). We aggregate via mean rank and top-2 counts (rank-1 and rank-2 placements) across all datasets. Statistical significance of rank differences is assessed with the Friedman test followed by Nemenyi post-hoc comparison at $\alpha = 0.05$ [13], automated via the `autorank` package [23]. The Nemenyi critical difference depends only on the number of models and datasets: $CD = 1.43$ for the full 8-model comparison ($k = 8$, $n = 54$) and $CD = 1.21$ for the CPU-viable 7-model comparison ($k = 7$, $n = 55$).

Computational setup. Outer CV folds are parallelised across CPU cores via `joblib`. To prevent thread thrashing, BLAS thread counts are pinned to 1 (OMP, MKL, and OpenBLAS environment variables) and model-internal parallelism is likewise disabled (`rf` and `xgb`: `n_jobs=1`). Wall-clock times for tuning, training, and prediction are recorded per fold to enable cost-accuracy trade-off analysis.

5 Results

This section reports results on accuracy and generalisation gap, together with computational cost. `tabPFN` is included throughout for completeness; given its deployment constraints (section 1), we also present CPU-viable rankings where relevant. Statistical comparisons use the Friedman test with Nemenyi post-hoc analysis described in section 4.5.

5.1 Predictive Accuracy

All models (with `tabPFN`). Figure 1a summarises predictive accuracy across 55 datasets for all eight models (full numerical results in table 7 in the appendix).⁴ `tabPFN` leads with 44 rank-1

⁴One dataset (`food_delivery_time`) is excluded from the 8-model comparison because `tabPFN` triggered a GPU out-of-memory error.

placements out of the 54 datasets on which it ran (one dataset excluded due to a GPU out-of-memory failure) and a mean rank of 1.49 (including a worst-rank penalty on the excluded dataset). Among the remaining models, `erbf`, `chebytree`, `xgb`, `chebypoly`, and `rf` form a statistically indistinguishable group (all pairwise rank differences within the Nemenyi critical difference), with mean ranks between 3.73 and 4.84. We refer to these five as the *competitive* models hereafter. `dt` and `ridge` form a separate lower group. Cross-dataset standard deviations of \bar{R}^2 are similar across the five competitive CPU models (0.22–0.23); `tabpfn`’s is slightly lower (0.20).

CPU-viable models (without `tabpfn`). Removing `tabpfn` (fig. 1b; numerical results in table 8 in the appendix) shifts the competition to the top of the ranking with all the top five models (`erbf`, `chebytree`, `xgb`, `chebypoly`, and `rf`) statistically tied. `erbf` achieves the best mean rank (2.84) with the most top-2 placements (12 wins, 15 runner-up), followed by `chebytree` (2.93; 8/13) and `xgb` (3.02; 17/8).

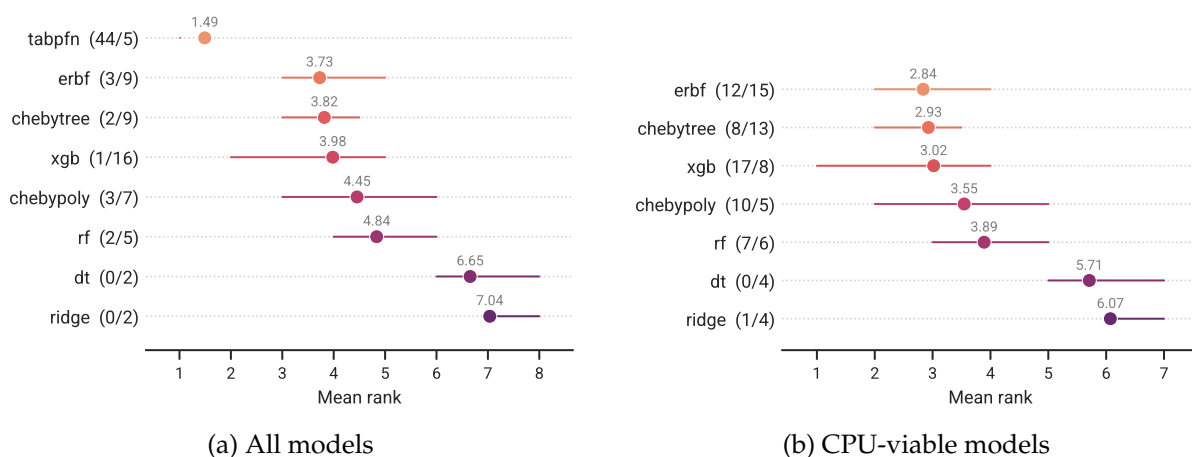


Figure 1: Mean rank for predictive accuracy (\bar{R}^2); parentheses show rank-1 wins / rank-2 places. Bars show the interquartile range of per-dataset ranks; CD bars indicate the Nemenyi critical difference (section 4.5): models whose mean ranks differ by less than CD are statistically indistinguishable. Full numerical results in tables 7 and 8 (appendix).

Figure 2 shows the full distribution of \bar{R}^2 across datasets for each model; the five competitive CPU-viable models have largely overlapping distributions.

Stratum-level analysis. Table 1 breaks down mean rank and \bar{R}^2 by domain stratum, examining whether model performance varies with the expected characteristics of the data-generating process (see section 4.4 for strata definitions).

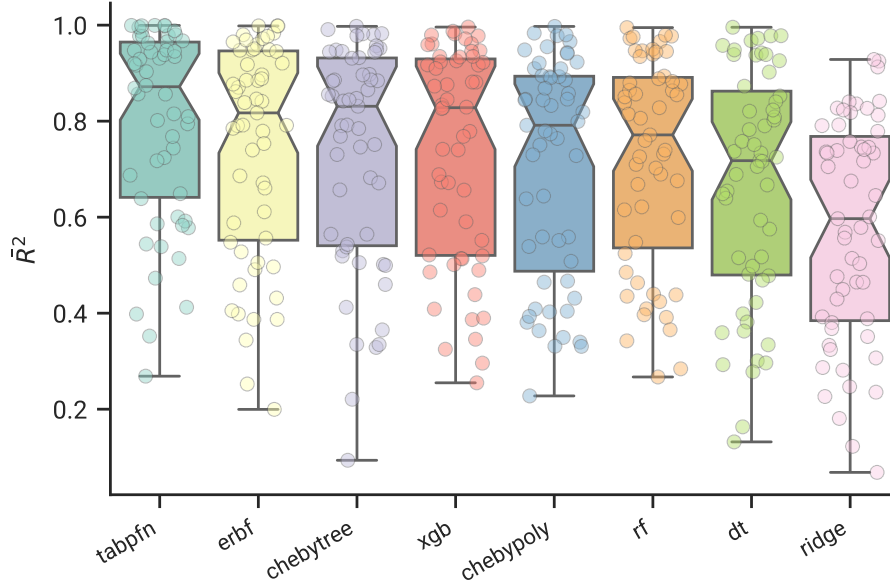


Figure 2: Distribution of \bar{R}^2 across 55 datasets per model (ordered by mean rank). Notched boxes show median and IQR; dots are individual datasets. The competitive cluster (ranks 2–6) has largely overlapping distributions, with the main separation occurring in the lower tail.

Table 1: Per-stratum mean rank and \bar{R}^2 (all models). Model order as in Figure 1a. Best CPU-viable model per stratum in **bold**, second underlined.

Model	S1 (13)		S2 (10)		S3 (16)		S4 (16)	
	Rank	\bar{R}^2	Rank	\bar{R}^2	Rank	\bar{R}^2	Rank	\bar{R}^2
tabpfn	1.38	0.947	1.89	0.618	1.19	0.723	1.25	0.852
erbf	3.08	0.921	4.80	0.549	3.50	0.657	3.81	0.809
chebytree	<u>3.69</u>	<u>0.903</u>	3.63	<u>0.555</u>	4.25	0.630	<u>3.62</u>	<u>0.813</u>
xgb	3.92	0.877	4.30	0.556	4.38	<u>0.651</u>	3.44	0.821
chebypoly	4.31	0.830	<u>4.00</u>	0.549	<u>4.06</u>	0.630	5.25	0.788
rf	5.54	0.871	4.50	0.551	4.56	0.636	4.75	0.793
dt	6.54	0.822	6.50	0.499	7.38	0.555	6.12	0.763
ridge	7.54	0.675	5.80	0.399	6.69	0.546	7.75	0.636

Among CPU-viable models, the stratification seems to provide a directional signal. *erbf* ranks best in S1 and S3 – the strata where physical or chemical processes suggest smoother target functions – while *xgb* leads in S4, where threshold-based pricing and policy rules could favour split-based models. S2 (behavioural/social data) shows lower accuracy across the board ($\bar{R}^2 \approx 0.40\text{--}0.62$), though *chebytree* leads (rank 3.63 vs. 4.00–4.80 for other competitive models), possibly reflecting the advantage of combining tree-based routing for discrete structure with smooth local fits within each partition.

The rank differences, however, are modest (typically less than one rank position between the top CPU-viable models), and the number of datasets per stratum (10–16) limits statistical power. The stratification should be read as a directional guide rather than a sharp prescription: it suggests which function class (smooth or piecewise-constant) is more likely to suit a given domain, without guaranteeing that a particular model will win. Grouping S1 and S3 into a “smooth” block (29 datasets) and S2 and S4 into a “threshold” block (26 datasets), *erbf* ranks first among CPU-viable models in the smooth block, while *xgb* and *chebytree* share the lead in

the threshold block. The hybrid chebytree is competitive across all four strata (rank 3.63–4.25), consistent with its capacity to combine tree-based regime detection with smooth local fits.

Effect of target discreteness. Thirteen of the 55 datasets have non-continuous regression targets: ordinal ratings and satisfaction scores (4–17 unique levels), integer counts (10–45 values), and measurements with a moderate number of distinct values (35–869 unique values). Table 2 compares mean ranks on continuous versus non-continuous targets.

Table 2: Mean rank by target type (CPU-viable models, excluding tabpfn). Non-continuous targets identified by systematic profiling of target cardinality and value structure. Best in **bold** per column among competitive models, second underlined.

Model	Continuous (42)	Non-continuous (13)	All (55)
erbf	2.50	3.92	2.84
chebytree	3.05	2.54	<u>2.93</u>
xgb	<u>2.90</u>	3.38	3.02
chebypoly	3.76	<u>2.85</u>	3.55
rf	3.86	4.00	3.89
dt	5.64	5.92	5.71
ridge	6.29	5.38	6.07

erbf shows the largest rank degradation on non-continuous targets: from 2.50 on continuous data to 3.92 (shift of +1.42), with zero wins on any non-continuous dataset. In contrast, chebypoly and chebytree both *improve* on non-continuous targets (shifts of -0.92 and -0.51 respectively), with chebytree ranking best (2.54).

A plausible architectural explanation is as follows. erbf’s localised Gaussian-like basis functions are a natural match for smooth targets but a poor one for step-like structure, which would require many narrow, overlapping bumps. chebypoly’s global polynomial basis can approximate piecewise structure through oscillation across the domain, reducing its sensitivity to discrete boundaries. chebytree is the most natural fit: its tree routing can partition the feature space into regions of roughly homogeneous target behaviour, while the smooth leaf polynomials handle variation within each partition. We note, however, that these are post-hoc rationalisations of the rank patterns; the benchmark does not isolate the mechanism. Restricting attention to the 42 continuous-target datasets sharpens the picture: erbf’s mean rank of 2.50 opens a 0.40 gap over the next-best model (xgb at 2.90), compared with just 0.09 overall, and all 12 of its wins come from this subset.

5.2 Generalisation Gap

The generalisation gap (training R^2 minus test R^2) quantifies how much of the training-set fit fails to transfer to held-out data, serving as a proxy for excess capacity beyond what the generalisable signal requires (section 1). Stability theory provides a formal link: models whose predictions change little when a single training example is replaced exhibit tighter generalisation bounds [5]. Figure 3 summarises the results (full numerical results in table 9 in the appendix). Note that ridge’s near-zero gap (median 0.004) is most likely a consequence of underfitting (high bias) rather than model quality.

Smooth and hybrid models (hereafter collectively ‘smooth models’ unless explicitly distinguished) exhibit substantially tighter generalisation gaps than tree ensembles. Among competitive models, chebypoly achieves the best gap rank (3.27, median gap 0.014), followed by erbf (3.84, median 0.018) and chebytree (4.29, median 0.025). xgb has the largest gap among competitive models (mean rank 7.31, median 0.079). The Nemenyi post-hoc test (section 4.5)

finds the following non-significant groups: {tabpfn, dt, rf, chebytree}; {dt, rf, chebytree, erbf}; {chebytree, erbf, chebypoly}. The difference between chebypoly and xgb (rank difference 4.04) is significant. tabpfn’s gap (median 0.047, rank 5.38) falls between dt and xgb, closer to the tree ensembles than to the smooth models; as a pre-trained model it has not been fitted to training data in the conventional sense, so its gap reflects the mismatch between its learned prior and each dataset rather than overfitting in the usual sense. A tighter gap indicates lower training-sample sensitivity: stability theory connects tighter gaps to bounded perturbation response [5], implying that such models depend less on the specific training sample. When accuracy is tied (within $0.02 \bar{R}^2$), smooth models win on gap in 87% of matched comparisons with tree ensembles (86/99 pairs across the four competitive pairings). The effect is strongest for chebypoly vs. xgb (22/23 datasets, 96%) and erbf vs. xgb (22/25, 88%), and holds against rf as well (chebypoly: 18/21, 86%; erbf: 24/30, 80%).

The few gap reversals are concentrated in S4 economic datasets (e.g., *Brazilian_houses*), where pricing tiers and policy thresholds may create genuinely piecewise-constant structure. A tree with a small number of well-placed splits can capture such structure at low effective complexity, yielding similar training and test performance; smooth models approximating the same discontinuities may require more basis functions, increasing effective complexity and with it the gap.

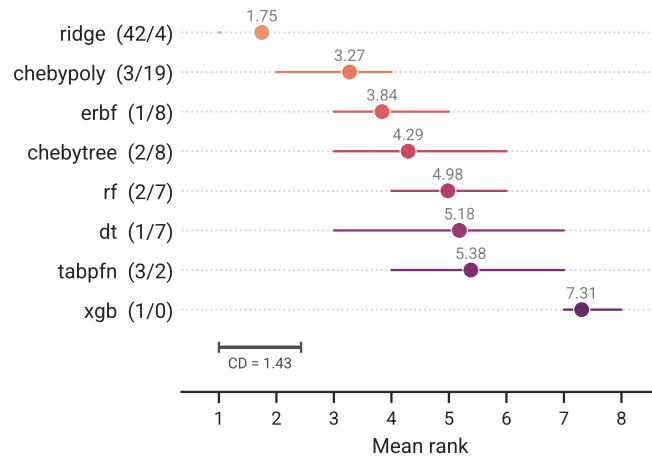


Figure 3: Mean rank for generalisation gap ($R_{\text{train}}^2 - R_{\text{test}}^2$); parentheses show rank-1 wins / rank-2 places; bars show the interquartile range. Lower rank = smaller gap. Smooth models (chebypoly, erbf) and the hybrid chebytree cluster at the top; xgb ranks last among competitive models. ridge’s top position reflects underfitting.

Accuracy-generalisation trade-off. Figure 4a plots each model in (\bar{R}^2, gap) space, treating lower gap as better for a given level of accuracy (fig. 4b shows the corresponding accuracy-cost trade-off). The Pareto front runs from ridge (lowest gap, lowest accuracy) through chebypoly and erbf to tabpfn (highest accuracy, moderate gap). Among CPU-viable models, the smooth-basis models occupy the best trade-off positions: erbf and chebypoly achieve competitive accuracy with substantially lower generalisation gaps than xgb or rf.

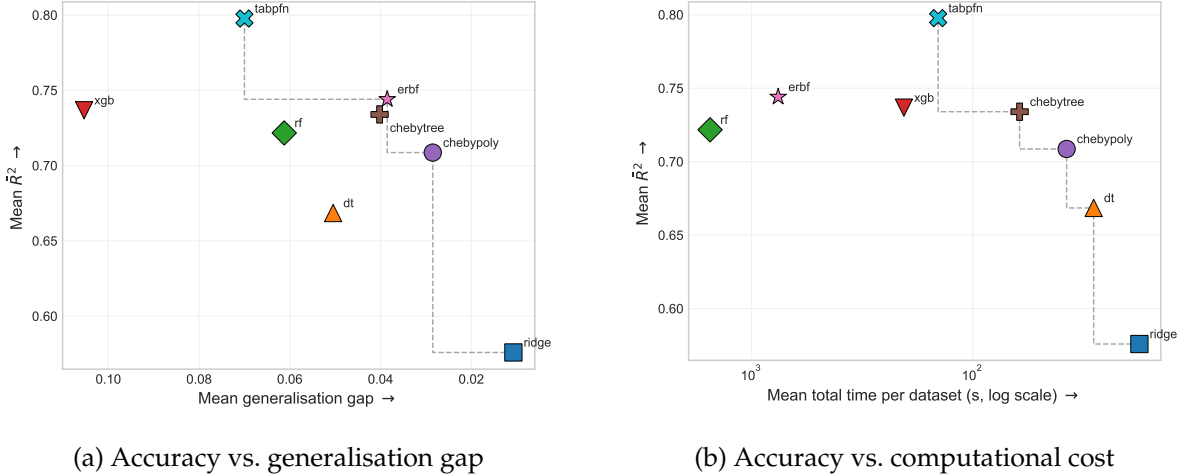


Figure 4: Pareto trade-off diagrams. Each point represents one model at its mean \bar{R}^2 plotted against (a) mean generalisation gap and (b) mean total time per dataset including tuning (log scale). Step lines trace the Pareto front; arrows on axes indicate the direction of improvement.

5.3 Computational Cost

Among the competitive CPU-viable models, chebypoly and chebytree are the cheapest to tune (37s and 61s mean, respectively), since their fitting reduces to ridge regression in the expanded basis. xgb (203s) is moderate; erbf (742s) and rf (1494s) are substantially more expensive, driven by L-BFGS-B width optimisation and full forest fitting per Optuna trial, respectively. tabpfn requires no tuning but incurs the highest prediction cost (5 131 ms per 1 000 instances) due to transformer inference, compared with under 50 ms for all other models except rf (229 ms). Once tuned, erbf offers fast inference (11 ms per 1 000 instances), competitive with xgb (17 ms). Full timing breakdowns are in tables 10 and 11 in the appendix.

The accuracy-cost Pareto front (fig. 4b) shows ridge, dt, chebypoly, and chebytree at the fast end; tabpfn extends it to the highest accuracy at moderate cost. erbf and rf fall off the front due to their higher tuning cost.

Scalability check. The main benchmark uses preprocessed data (at most 50 features and 50 000 samples) to accommodate tabpfn’s input constraints and the computational cost of erbf and rf tuning at high dimensionality. To test whether the Chebyshev models remain competitive at full scale, we ran the five scalable models (ridge, dt, xgb, chebypoly, and chebytree) on eight datasets without any feature selection or sample subsampling, including datasets with up to $n = 581,835$ samples and $d = 1,024$ features (table 3).

On this small sample, chebytree matches xgb closely (mean \bar{R}^2 0.765 vs. 0.769) and wins on three of the eight datasets; chebypoly scores lower (0.728) but remains ahead of ridge and dt. These results suggest that both Chebyshev models can scale to full-size data without feature selection or subsampling, though the limited number of datasets precludes strong conclusions.

The distribution of winning hyperparameter configurations across the 55 datasets is reported in section D.

5.4 Practical Model Selection

The preceding subsections evaluated models along individual axes – accuracy, generalisation gap, and computational cost. Here we draw these threads together into practical guidance for

Table 3: Scalability check: \bar{R}^2 per dataset for scalable models on full-scale data (no feature selection or subsampling). Datasets ordered by mean \bar{R}^2 across models. Best per dataset in **bold**.

Dataset	S	n	d	xgb	chebytree	chebypoly	ridge	dt
medical_charges	S4	163K	3	0.978	0.980	0.979	0.825	0.978
diamonds	S4	54K	6	0.946	0.945	0.943	0.926	0.942
superconduct	S3	21K	79	0.910	0.900	0.837	0.733	0.825
friedman1_d100	S1	2K	100	0.926	0.878	0.905	0.710	0.676
geo_music	S2	1K	117	0.647	0.670	0.758	0.756	0.473
qsar_tid_11	S3	6K	1024	0.611	0.634	0.523	0.538	0.265
allstate_claims	S4	188K	130	0.547	0.549	0.482	0.494	0.428
nyc_taxi	S4	582K	9	0.588	0.567	0.398	0.308	0.513
<i>Mean</i>				0.769	0.765	0.728	0.661	0.637

model selection. No single model dominates all criteria, and the best choice depends on which trade-offs matter most for a given application; all competitive families should be benchmarked on the target problem. What follows are empirically grounded priors to inform that process.

Domain knowledge can inform priors about which family to favour. The stratum analysis (section 5.1) offers a directional guide: smooth models tend to rank higher on datasets from engineering, simulation, and physical-science domains (S1, S3), while tree ensembles tend to lead on economic and pricing datasets with threshold-driven structure (S4). These are tendencies, not guarantees (section 4.4).

When models achieve comparable accuracy on a given problem – which, given the aggregate tie, can often be the case – other criteria become decisive. The matched-accuracy gap advantage (87% of pairwise comparisons, section 5.2) and the accuracy-gap Pareto front (fig. 4a) both favour smooth models. Depending on the application, a practitioner may also choose to accept a small accuracy trade-off in favour of smooth prediction surfaces (for surrogate optimisation or sensitivity analysis), structural interpretability, or lower computational cost.

On computational cost (section 5.3), chebypoly and chebytree are the fastest competitive models, placing them on the accuracy-cost Pareto front (fig. 4b). erbf and rf fall off this front due to expensive tuning, though erbf’s fast inference (table 10) means the tuning cost is a one-time investment amortised over subsequent predictions.

Scalability further differentiates the models. The scalability check (table 3) showed that xgb, chebytree, and chebypoly all run at full scale without preprocessing, though the Chebyshev basis size grows combinatorially with dimensionality. erbf’s $O(nKd)$ per-iteration cost makes it the most expensive smooth model to tune at high n or d . tabPFN requires GPU memory proportional to n^2 and is capped at 50K samples, making it best suited to moderate-sized problems where GPU inference is available.

Smooth models also offer a degree of structural interpretability not shared by tree ensembles. chebypoly yields explicit polynomial coefficients from which partial derivatives and sensitivity indices can be computed; chebytree combines tree routing with local polynomial coefficients; erbf provides geometric interpretability via localised basis functions whose widths indicate local feature relevance. xgb and rf are more commonly interpreted through post-hoc tools (SHAP, partial dependence), though these tools are equally applicable to smooth models. These are structural properties of the model architectures; a comparative evaluation of interpretability is beyond the scope of this benchmark. As noted in section 1, smooth prediction surfaces are additionally valuable when outputs feed into gradient-based optimisation or sensitivity analysis.

In summary, when generalisation gap and interpretability are priorities, `erbf` and `chebypoly` offer the strongest profiles among CPU-viable models. When tuning budget is limited, `chebytree` and `chebypoly` provide competitive accuracy at the lowest cost. When scalability to high-dimensional data is the binding constraint, `xgb` and `chebytree` both proved viable at full scale. Tabular deep learning models such as `tabpfn` can extend the accuracy frontier further, subject to the GPU memory and inference latency constraints typical of this model family.

6 Discussion

Limitations. Several considerations qualify the conclusions of this study.

The benchmark is restricted to regression. Classification tasks, which dominate many tabular benchmarks, may favour different model families.

Our evaluation uses a fixed nested cross-validation protocol with Optuna-based hyperparameter tuning. Trial budgets (20–50 per model, proportional to search space dimensionality) were chosen to keep resource usage comparable across models; more trials could shift relative rankings, particularly for `erbf`, whose width optimisation involves a non-convex inner loop that benefits from broader search.

The main preprocessing pipeline applies mutual-information-based feature selection (capping at 50 features) and sample subsampling (capping at 50 000 instances) to keep tuning tractable across all models and to satisfy `tabpfn`'s input constraints. Although these caps are applied uniformly, their effect on different model families is not necessarily symmetric. The scalability check (table 3) partially addresses this by running scalable models on full-scale data without preprocessing, but a complete comparison at full scale for all models would require substantially more computation. Relatedly, we applied a uniform preprocessing pipeline across all datasets rather than tailoring feature engineering to each domain; domain-specific feature construction (e.g. task-specific molecular fingerprints instead of generic RDKit descriptors) might improve all models. Results on individual datasets should therefore be interpreted as reflecting the model-pipeline combination, not the model alone.

All train-from-scratch models in the benchmark operate in axis-aligned feature coordinates: trees splits act on single features, ERBF uses diagonal (per-dimension) widths, and Chebyshev interaction terms are products along coordinate axes. Data with strong oblique structure (relationships aligned along linear combinations of features) may disadvantage all families equally; preprocessing such as PCA rotation could benefit all models.

We evaluated 55 datasets from four domain strata, a number that is large by the standards of tabular regression benchmarks but still insufficient to make definitive claims about specific application domains. The stratum-level analysis (section 5.1) is exploratory rather than confirmatory.

Future work. Extending the evaluation to classification is the most natural next step. Formal assessment of prediction-surface regularity, for example via local Lipschitz analysis, could complement the generalisation gap analysis presented here. For ERBF specifically, scaling the $O(nKd)$ per-iteration cost via mini-batch optimisation or sparse activations remains an open direction. Hybrid architectures that combine tree-based routing with local smooth fits, or target transformations that map discrete outcomes to a continuous latent space, could address ERBF's sensitivity to non-continuous targets.

Broader implications. The accuracy-gap trade-off documented in section 5.4 has implications beyond the specific models and datasets studied here. Our exploratory stratum analysis (section 5.1) offers a tentative counterpoint to the established narrative that tree ensembles dominate tabular data. Smooth models lead in the engineering and natural-science strata (S1, S3),

and even in the economics and behavioural strata (S2, S4) – where threshold-driven targets might favour split-based models – tree ensembles hold only a narrow lead or none at all. The strata are based on domain judgement rather than formal criteria, and the per-stratum sample sizes are small, so these patterns should be read as suggestive rather than conclusive. They do, however, hint that the dominance of tree ensembles may be less universal than benchmark leaderboards – which draw heavily from commercial and administrative domains – suggest. More broadly, evaluating generalisation gap alongside accuracy is informative because models that achieve similar held-out scores can differ substantially in their sensitivity to the specific training sample, and a tighter gap signals lower such sensitivity [5].

The practical benefits of smooth prediction surfaces extend beyond the benchmark setting. In surrogate-based engineering design, an optimiser that follows the surrogate’s gradient may become trapped or oscillate when the surface contains artefactual discontinuities at tree-split boundaries; the optimiser chases model structure rather than genuine improvements in the objective – a practical consideration that motivates the use of smooth surrogates in model-based optimisation [16, 27]. In consumer-facing applications such as loan calculators or insurance quotations, users expect that small changes to inputs produce proportionate changes in outputs; a split boundary that causes a large price jump for a negligible input change undermines trust. These settings do not require certified smoothness guarantees, but they benefit from prediction surfaces that vary gradually.

The evaluation framework developed here – combining accuracy, generalisation gap, and computational cost – is applicable to any regression model and could serve as a template for future tabular benchmarks. The generalisation advantage we observe may extend to other model families that produce smooth prediction surfaces, though this remains to be tested.

7 Conclusion

We have benchmarked two smooth-basis model families (Chebyshev polynomial regressors and anisotropic RBF networks) and a smooth-tree hybrid (Chebyshev model trees) against tree ensembles and a pre-trained transformer across 55 tabular regression datasets, evaluating predictive accuracy and generalisation behaviour.

The main finding is that smooth-basis models match tree ensembles on predictive accuracy while tending to generalise better: the five competitive CPU-viable models are statistically indistinguishable on accuracy, but smooth models exhibit tighter generalisation gaps in the large majority of pairwise comparisons at matched accuracy (section 5.4).

These results do not argue that smooth models should replace tree ensembles universally; model selection depends on the balance of aspects including accuracy, generalisation, cost, and interpretability for each application (section 5.4). Rather, they suggest that smooth models deserve routine inclusion in the candidate pool, and that the practitioner’s default of gradient-boosted trees, while reasonable, could leave potential gains in other evaluative axes on the table. When two models achieve comparable accuracy, for example, one could favour the one with the tighter generalisation gap.

Reproducibility. All experiments use fixed random seeds (outer CV seed 42, Optuna seed 0) and deterministic nested cross-validation splits. The model implementations are available on PyPI (`pip install erbf poly-basis-ml`), and the full benchmark code—including analysis scripts, dataset loaders, and result summaries—is available at <https://github.com/gerber1/poly-erbf-benchmark>. The benchmark was run with Python 3.12, scikit-learn 1.6, XGBoost 3.1, Optuna 4.6, and NumPy 2.3; a complete environment specification (`environment.yml`) is included in the repository. Datasets are drawn from OpenML, UCI, PMLB, MoleculeNet, Hugging Face Datasets, scikit-learn generators, and custom synthetic functions (sources and IDs

listed in section F). Experiments were conducted on a workstation with an Intel Core i9-9900X CPU (10 cores, 20 threads, 3.50 GHz), 128 GB RAM, and an NVIDIA TITAN RTX GPU (24 GB VRAM), running Linux 6.1. Hyperparameter search spaces are fully specified in section B, and per-dataset results are reported in section F.

References

- [1] Rishabh Agarwal, Levi Melnick, Nicholas Frosst, Xuezhou Zhang, Ben Lengerich, Rich Caruana, and Geoffrey E. Hinton. Neural additive models: Interpretable machine learning with neural nets. In *Advances in Neural Information Processing Systems*, volume 34, 2021.
- [2] Takuya Akiba, Shotaro Sano, Toshihiko Yanase, Takeru Ohta, and Masanori Koyama. Optuna: A next-generation hyperparameter optimization framework. In *Proceedings of the 25th ACM SIGKDD International Conference on Knowledge Discovery and Data Mining*, pages 2623–2631, 2019.
- [3] Sercan Ö. Arik and Tomas Pfister. TabNet: Attentive interpretable tabular learning. In *Proceedings of the AAAI Conference on Artificial Intelligence*, volume 35, pages 6679–6687, 2021.
- [4] Mikhail Belkin, Daniel Hsu, Siyuan Ma, and Soumik Mandal. Reconciling modern machine-learning practice and the classical bias–variance trade-off. *Proceedings of the National Academy of Sciences*, 116(32):15849–15854, 2019.
- [5] Olivier Bousquet and André Elisseeff. Stability and generalization. *Journal of Machine Learning Research*, 2:499–526, 2002.
- [6] Leo Breiman. Random forests. *Machine Learning*, 45(1):5–32, 2001.
- [7] David S. Broomhead and David Lowe. Radial basis functions, multi-variable functional interpolation and adaptive networks. *Royal Signals and Radar Establishment Memorandum*, (4148), 1988.
- [8] Martin D. Buhmann. *Radial Basis Functions: Theory and Implementations*. Cambridge University Press, 2003. doi: 10.1017/CBO9780511543241.
- [9] Richard H. Byrd, Peihuang Lu, Jorge Nocedal, and Ciyou Zhu. A limited memory algorithm for bound constrained optimization. *SIAM Journal on Scientific Computing*, 16(5): 1190–1208, 1995.
- [10] Gavin C. Cawley and Nicola L. C. Talbot. On over-fitting in model selection and subsequent selection bias in performance evaluation. *Journal of Machine Learning Research*, 11: 2079–2107, 2010.
- [11] Sheng Chen, Colin F. N. Cowan, and Peter M. Grant. Orthogonal least squares learning algorithm for radial basis function networks. *IEEE Transactions on Neural Networks*, 2(2): 302–309, 1991.
- [12] Tianqi Chen and Carlos Guestrin. XGBoost: A scalable tree boosting system. In *Proceedings of the 22nd ACM SIGKDD International Conference on Knowledge Discovery and Data Mining*, pages 785–794, 2016.
- [13] Janez Demšar. Statistical comparisons of classifiers over multiple data sets. *Journal of Machine Learning Research*, 7:1–30, 2006.

- [14] Dheeru Dua and Casey Graff. UCI machine learning repository, 2017. URL <https://archive.ics.uci.edu/ml>.
- [15] Manuel Fernández-Delgado, Eva Cernadas, Senén Barro, and Dinani Amorim. Do we need hundreds of classifiers to solve real world classification problems? *Journal of Machine Learning Research*, 15(1):3133–3181, 2014.
- [16] Alexander I. J. Forrester and Andy J. Keane. Recent advances in surrogate-based optimization. *Progress in Aerospace Sciences*, 45(1–3):50–79, 2009.
- [17] Jerome H. Friedman. Multivariate adaptive regression splines. *The Annals of Statistics*, 19(1):1–67, 1991.
- [18] Yury Gorishniy, Ivan Rubachev, Valentin Khruikov, and Artem Babenko. Revisiting deep learning models for tabular data. In *Advances in Neural Information Processing Systems*, volume 34, 2021.
- [19] Léo Grinsztajn, Edouard Oyallon, and Gaël Varoquaux. Why do tree-based models still outperform deep learning on typical tabular data? In *Advances in Neural Information Processing Systems*, volume 35, pages 507–520, 2022.
- [20] Léo Grinsztajn, Klemens Flöge, Oscar Key, Felix Birkel, Philipp Jund, Brendan Roof, Benjamin Jäger, Dominik Safaric, Simone Alessi, Adrian Hayler, Mihir Manium, Rosen Yu, Felix Jablonski, Shi Bin Hoo, Anurag Garg, Jake Robertson, Magnus Bühler, Vladyslav Moroshan, Lennart Purucker, Clara Cornu, Lilly Charlotte Wehrhahn, Alessandro Bonetto, Bernhard Schölkopf, Sauraj Gambhir, Noah Hollmann, and Frank Hutter. TabPFN-2.5: Advancing the state of the art in tabular foundation models, 2025. URL <https://arxiv.org/abs/2511.08667>.
- [21] Charles R. Harris, K. Jarrod Millman, Stéfan J. van der Walt, Ralf Gommers, Pauli Virtanen, David Cournapeau, Eric Wieser, Julian Taylor, Sebastian Berg, Nathaniel J. Smith, Robert Kern, Matti Picus, Stephan Hoyer, Marten H. van Kerevelen, Matthew Brett, Allan Haldane, Jaime Fernández del Río, Mark Wiebe, Pearu Peterson, Pierre Gérard-Marchant, Kevin Sheppard, Tyler Reddy, Warren Weckesser, Hameer Abbasi, Christoph Gohlke, and Travis E. Oliphant. Array programming with NumPy. *Nature*, 585:357–362, 2020.
- [22] Trevor J. Hastie and Robert J. Tibshirani. *Generalized Additive Models*. Chapman and Hall, 1990.
- [23] Steffen Herbold. Autorank: A Python package for automated ranking of classifiers. *Journal of Open Source Software*, 5(48):2173, 2020. doi: 10.21105/joss.02173.
- [24] Arthur E. Hoerl and Robert W. Kennard. Ridge regression: Biased estimation for nonorthogonal problems. *Technometrics*, 12(1):55–67, 1970.
- [25] Noah Hollmann, Samuel Müller, Lennart Purucker, Arjun Krishnakumar, Max Körfer, Shi Bin Hoo, Robin Tibor Schirrmeyer, and Frank Hutter. Accurate predictions on small data with a tabular foundation model. *Nature*, 2025. doi: 10.1038/s41586-024-08328-6.
- [26] John D. Hunter. Matplotlib: A 2D graphics environment. *Computing in Science & Engineering*, 9(3):90–95, 2007.
- [27] Donald R. Jones, Matthias Schonlau, and William J. Welch. Efficient global optimization of expensive black-box functions. *Journal of Global Optimization*, 13(4):455–492, 1998.

- [28] Siu Kwan Lam, Antoine Pitrou, and Stanley Seibert. Numba: A LLVM-based Python JIT compiler. *Proceedings of the Second Workshop on the LLVM Compiler Infrastructure in HPC*, pages 1–6, 2015.
- [29] Greg Landrum. RDKit: Open-source cheminformatics software, 2016. URL <https://www.rdkit.org>. <https://www.rdkit.org>.
- [30] Ziming Liu, Yixuan Wang, Sachin Vaidya, Fabian Ruehle, James Halverson, Marin Soljačić, Thomas Y. Hou, and Max Tegmark. KAN: Kolmogorov–Arnold networks. In *International Conference on Learning Representations*, 2025.
- [31] Duncan McElfresh, Sujay Khandagale, Jonathan Valverde, Vishak Prasad C, Benjamin Feuer, Chinmay Hegde, Ganesh Ramakrishnan, Micah Goldblum, and Colin White. When do neural nets outperform boosted trees on tabular data? In *Advances in Neural Information Processing Systems*, volume 36, 2023.
- [32] Harsha Nori, Samuel Jenkins, Paul Koch, and Rich Caruana. InterpretML: A unified framework for machine learning interpretability. *arXiv preprint arXiv:1909.09223*, 2019.
- [33] Fabian Pedregosa, Gaël Varoquaux, Alexandre Gramfort, Vincent Michel, Bertrand Thirion, Olivier Grisel, Mathieu Blondel, Peter Prettenhofer, Ron Weiss, Vincent Dubourg, Jake Vanderplas, Alexandre Passos, David Cournapeau, Matthieu Brucher, Matthieu Perrot, and Édouard Duchesnay. Scikit-learn: Machine learning in Python. *Journal of Machine Learning Research*, 12:2825–2830, 2011.
- [34] Tomaso Poggio and Federico Girosi. Networks for approximation and learning. *Proceedings of the IEEE*, 78(9):1481–1497, 1990.
- [35] Sergei Popov, Stanislav Morozov, and Artem Babenko. Neural oblivious decision ensembles for deep learning on tabular data. In *International Conference on Learning Representations*, 2020.
- [36] Jingang Qu, David Holzmüller, Gaël Varoquaux, and Marine Le Morvan. TabICL: A tabular foundation model for in-context learning on large data. In *Proceedings of the 42nd International Conference on Machine Learning*, 2025.
- [37] J. Ross Quinlan. Learning with continuous classes. In *Proceedings of the 5th Australian Joint Conference on Artificial Intelligence*, pages 343–348, 1992.
- [38] Carl Edward Rasmussen and Christopher K. I. Williams. *Gaussian Processes for Machine Learning*. MIT Press, 2006.
- [39] Joseph D. Romano, Trang T. Le, William La Cava, John T. Greber, Daniel E. Goldberg, and Jason H. Moore. PMLB v1.0: An open-source dataset collection for benchmarking machine learning methods. *Bioinformatics*, 38(3):878–880, 2022.
- [40] Ravid Shwartz-Ziv and Amitai Armon. Tabular data: Deep learning is not all you need. *Information Fusion*, 81:84–90, 2022.
- [41] The Joblib Developers. Joblib, 2025. URL <https://github.com/joblib/joblib>.
- [42] Michalis K. Titsias. Variational learning of inducing variables in sparse Gaussian processes. In *Proceedings of the 12th International Conference on Artificial Intelligence and Statistics*, pages 567–574, 2009.
- [43] Lloyd N. Trefethen. *Approximation Theory and Approximation Practice, Extended Edition*. SIAM, 2019.

- [44] Joaquin Vanschoren, Jan N. van Rijn, Bernd Bischl, and Luís Torgo. OpenML: Networked science in machine learning. *SIGKDD Explorations*, 15(2):49–60, 2014.
- [45] Pauli Virtanen, Ralf Gommers, Travis E. Oliphant, Matt Haberland, Tyler Reddy, David Cournapeau, Evgeni Burovski, Pearu Peterson, Warren Weckesser, Jonathan Bright, Stéfan J. van der Walt, Matthew Brett, Joshua Wilson, K. Jarrod Millman, Nikolay Mayorov, Andrew R. J. Nelson, Eric Jones, Robert Kern, Eric Larson, C. J. Carey, İlhan Polat, Yu Feng, Eric W. Moore, Jake VanderPlas, Denis Laxalde, Josef Perktold, Robert Cimrman, Ian Henriksen, E. A. Quintero, Charles R. Harris, Anne M. Archibald, Antônio H. Ribeiro, Fabian Pedregosa, Paul van Mulbregt, and SciPy 1.0 Contributors. SciPy 1.0: Fundamental algorithms for scientific computing in Python. *Nature Methods*, 17:261–272, 2020.
- [46] Yong Wang and Ian H. Witten. Induction of model trees for predicting continuous classes. *Working Paper Series, Department of Computer Science, University of Waikato*, (96/23), 1997.
- [47] Michael L. Waskom. seaborn: statistical data visualization. *Journal of Open Source Software*, 6(60):3021, 2021.
- [48] Zhenqin Wu, Bharath Ramsundar, Evan N. Feinberg, Joseph Gomes, Caleb Geniesse, Anurag S. Pappu, Karl Leswing, and Vijay Pande. MoleculeNet: A benchmark for molecular machine learning. *Chemical Science*, 9(2):513–530, 2018.
- [49] Yuguo Zhou, Tong Mu, Zhong-Hua Pang, and Changbing Zheng. A survey on hyper basis function neural networks. *Systems Science & Control Engineering*, 7(1):399–415, 2019. doi: 10.1080/21642583.2019.1699474.
- [50] Hui Zou and Trevor Hastie. Regularization and variable selection via the elastic net. *Journal of the Royal Statistical Society: Series B (Statistical Methodology)*, 67(2):301–320, 2005.

A ERBF Training Pipeline

Algorithm 1 Three-stage ERBF training pipeline.

Require: Training data $\{(\mathbf{x}_i, y_i)\}_{i=1}^n$, number of centres K , ridge penalty α , neighbourhood size k_{nn}

Ensure: Centres $\{\mathbf{c}_k\}$, widths $\{\sigma_k\}$, weights $\{w_k\}$, bias b

Stage 1: Centre placement

▷ Hyperparameter: center_init

1: **if** Lipschitz-guided (default) **then**

2: **for** $i = 1, \dots, n$ **do**

3: Compute local Lipschitz constant $L_i = \max_{j \in \text{kNN}(i)} \frac{|y_i - y_j|}{\|\mathbf{x}_i - \mathbf{x}_j\| + \epsilon}$

4: **end for**

5: Clip L_i at the 99th percentile

6: Sample K centres $\{\mathbf{c}_k\}$ from training points without replacement, with $P(\mathbf{x}_i) \propto L_i$

7: **else if** K -means **then**

8: Run K -means on training features \rightarrow centroids $\{\mathbf{c}_k\}$

9: **end if**

Stage 2: Width initialisation

▷ Hyperparameter: width_init

10: **for** $k = 1, \dots, K$ **do**

11: Find k_{nn} nearest neighbours of \mathbf{c}_k

12: **if** Local ridge (default) **then**

13: Fit local ridge regression \rightarrow coefficients β_j

14: Set $\sigma_{kj}^2 \leftarrow \text{Var}_{\text{local}}(x_j) / |\beta_j|$ for $j = 1, \dots, d$

15: **else if** Local variance **then**

16: Set $\sigma_{kj} \leftarrow \text{std}_{\text{local}}(x_j) \cdot \sqrt{d}$ for $j = 1, \dots, d$

17: **end if**

18: **end for**

Stage 3: Width optimisation

19: $\theta \leftarrow \log \sigma$

▷ Enforce positivity via log-space

20: $\theta^* \leftarrow \text{L-BFGS-B}(\min_{\theta} \frac{1}{n} \sum_{i=1}^n (y_i - f(\mathbf{x}_i))^2, \theta_0 = \theta, \text{maxiter} = 30)$

21: $\sigma \leftarrow \exp(\theta^*)$

Output weights

22: Compute activation matrix $\Phi \in \mathbb{R}^{n \times K}$ with $\Phi_{ik} = \phi_k(\mathbf{x}_i)$

▷ Eq. 1

23: $\mathbf{w} \leftarrow (\Phi^T \Phi + \alpha \mathbf{I})^{-1} \Phi^T \mathbf{y}$

▷ $\mathbf{I} \in \mathbb{R}^{K \times K}$ identity matrix

B Hyperparameter Search Spaces

Table 4 lists the full per-model search spaces used by Optuna during the inner loop of nested cross-validation. All continuous regularisation parameters are sampled on a log-uniform scale; structural parameters (depths, counts) use uniform integer sampling; algorithmic variants use categorical sampling. Fixed (non-tuned) settings are shown as greyed rows.

Table 4: Hyperparameter search spaces and fixed settings for each model. “Log” indicates log-uniform sampling; “Cat” indicates categorical. Trial budgets are given in parentheses after each model name. Greyed rows show fixed (non-tuned) settings.

Model	Parameter	Range / choices	Scale
Ridge (20 trials)	alpha	$[10^{-3}, 10^3]$	Log
Decision Tree (25 trials)	max_depth	[1, 20]	Int
	min_samples_leaf	[0.005, 0.1]	Uniform
	min_samples_split	[0.01, 0.1]	Uniform
Random Forest (25 trials)	n_estimators	[50, 500]	Int
	max_depth	[3, 20]	Int
	max_features	{0.3, 0.5, 0.7, sqrt}	Cat
	min_samples_leaf	0.005	Fixed
XGBoost (50 trials)	max_depth	[1, 9]	Int
	learning_rate	[0.01, 0.3]	Log
	subsample	[0.6, 1.0]	Uniform
	colsample_bytree	[0.6, 1.0]	Uniform
	reg_lambda	$[10^{-3}, 10^3]$	Log
	min_child_weight	[1, 100]	Log
	n_estimators	2 000 (early stop, patience 10)	Fixed
	validation split	15% of training set	Fixed
ERBF (30 trials)	n_rbf	{auto} \cup [10, 80]	Cat / Int
	alpha	$[10^{-3}, 10^3]$	Log
	center_init	{lipschitz, kmeans}	Cat
	width_init	{local_ridge, local_variance}	Cat
	width_optim_iters	30	Fixed
	width_mode	full (gradient-based)	Fixed
ChebyPoly (30 trials)	complexity	[1, 14]	Int
	alpha	$[10^{-3}, 10^3]$	Log
	include_interactions	{True, False}	Cat
	max_interaction_complexity	{1, 2}	Cat [†]
	solver / clip_input	Ridge; True	Fixed
	interaction_types	[product]	Fixed
ChebyTree (30 trials)	complexity	[1, 6]	Int
	alpha	$[10^{-3}, 10^3]$	Log
	max_depth	[1, 12]	Int
	min_samples_leaf	[0.01, 0.1]	Uniform
	solver	Ridge	Fixed
tabpfn (0 trials)	Zero-shot; no hyperparameters tuned.		

[†] Conditional on include_interactions = True. All stochastic models use random_state = 42.

C Dataset Catalogue

Table 5: All 55 benchmark datasets grouped by stratum. n = samples, d = features, n' and d' = effective counts after preprocessing (shown only where they differ from n/d). Datasets with non-continuous targets are marked[†] (13 total; see table 2). Data URLs are hyperlinked in the electronic version.

Dataset	n	d	n'	d'	Source	Data URL
S1 – Engineering/Simulation (13 datasets)						
airfoil_noise	1 503	5			UCI	uci.edu/dataset/291
Ailerons [†]	13 750	33	30		OpenML	openml.org/d/44137
concrete_strength	1 030	8			UCI	uci.edu/dataset/165
cpu_act [†]	8 192	21			OpenML	openml.org/d/44132
elevators [†]	16 599	16			OpenML	openml.org/d/44134
energy_efficiency_heating	768	8			UCI	uci.edu/dataset/242
feynman_gaussian	8 000	2			HF	srsd-feynman_hard
feynman_wave_interference	8 000	4			HF	srsd-feynman_hard
friedman1	2 000	5			sklearn	make_friedman1
friedman1_d100	2 000	100	16		sklearn	make_friedman1
pmlb_215_2dplanes	40 768	10			PMLB	215_2dplanes
pmlb_225_puma8NH	8 192	8			PMLB	225_puma8NH
power_plant	9 568	4			UCI	uci.edu/dataset/294
S2 – Behavioural/Social (10 datasets)						
analcatsdata_supreme [†]	4 052	7	5		OpenML	openml.org/d/504
Bike_Sharing_Demand	17 379	6			OpenML	openml.org/d/44142
food_delivery_time [†]	45 451	9			OpenML	openml.org/d/46928
pmlb_1028_SWD [†]	1 000	10			PMLB	1028_SWD
pmlb_1029_LEV [†]	1 000	4			PMLB	1029_LEV
pmlb_1030_ERA [†]	1 000	4			PMLB	1030_ERA
pmlb_4544_GeoMusic	1 059	117	50		PMLB	4544_Geo...Music
pol [†]	15 000	26	16		OpenML	openml.org/d/44133
student_performance [†]	649	30	29		UCI	uci.edu/dataset/320
wine_quality [†]	6 497	11			OpenML	openml.org/d/44136
S3 – Physics/Chemistry/Life Sciences (16 datasets)						
abalone [†]	4 177	7			HF	tabular-benchmark
diabetes	442	10			sklearn	load_diabetes
esol	1 128	7			MolNet	moleculenet.org
freesolv	642	16	13		MolNet	moleculenet.org
lipophilicity	4 200	16	13		MolNet	moleculenet.org
particulate-matter	394 299	9	50K		OpenML	openml.org/d/42207
physiochem_protein	45 730	9			OpenML	openml.org/d/46949
pmlb_503_wind	6 574	14			PMLB	503_wind
pmlb_522_pm10	500	7			PMLB	522_pm10
pmlb_529_pollen	3 848	4			PMLB	529_pollen
pmlb_547_no2	500	7			PMLB	547_no2
qm7	6 834	16	14		MolNet	moleculenet.org
qsar_fish_toxicity	907	6			OpenML	openml.org/d/46954
qsar_tid_11	5 742	1 024	50		OpenML	openml.org/d/46953
sulfur	10 081	6			OpenML	openml.org/d/44145
superconduct	21 263	79	50		OpenML	openml.org/d/44148
S4 – Economic/Pricing (16 datasets)						
Allstate_Claims	188 318	130	50K	50	OpenML	openml.org/d/42571
Brazilian_houses	10 692	8			OpenML	openml.org/d/44141
california_housing	20 640	8			sklearn	fetch_california_housing
diamonds	53 940	6	50K		OpenML	openml.org/d/44140
fiat_500_price	1 538	7			OpenML	openml.org/d/46907
healthcare_insurance	1 338	6			OpenML	openml.org/d/46931
house_16H	22 784	16			OpenML	openml.org/d/44139

Continued on next page

Dataset	n	d	n'	d'	Source	Data URL
house_sales	21 613	15		14	OpenML	openml.org/d/44144
medical_charges	163 065	3	50K		OpenML	openml.org/d/44146
MiamiHousing2016	13 932	13			OpenML	openml.org/d/44147
nyc-taxi [†]	581 835	9	50K	8	OpenML	openml.org/d/44143
pmlb_218_house_8L	22 784	8			PMLB	218_house_8L
power_grid_stability	10 000	12			UCI	uci.edu/dataset/471
synthetic_multithreshold	750	6			synth.	this study ^a
synthetic_piecewise	2 000	5			synth.	this study ^b
synthetic_step	2 000	8			synth.	this study ^c

[†] Non-continuous target (ordinal, integer-valued, or discrete-like); see table 2 for details. Treated as continuous regression throughout. All synthetic targets include additive Gaussian noise ϵ .

$$^a y = 3\mathbf{1}[x_0 > 0] + 2\mathbf{1}[x_1 > 0.5] + 1.5\mathbf{1}[x_2 < -0.3] + \mathbf{1}[|x_3| < 1] + 0.5\mathbf{1}[x_0 > 0]\mathbf{1}[x_1 > 0] + \epsilon$$

$$^b y = 2[x_0]_+ + 1.5[-x_1]_+ + [x_2 - 0.5]_+ - [x_0 + x_1]_+ + \epsilon$$

$$^c y = 2\mathbf{1}[x_0 > 0] + 3\mathbf{1}[x_1 > 0.5] - 1.5\mathbf{1}[x_2 < -0.5] + \mathbf{1}[x_0 > 0]\mathbf{1}[x_1 > 0] + \epsilon$$

Source key. UCI = UCI Machine Learning Repository; OpenML = OpenML repository; PMLB = Penn Machine Learning Benchmarks; MolNet = MoleculeNet; HF = Hugging Face Datasets; sklearn = scikit-learn datasets module; synth. = generated by this study. All Data URL entries are hyperlinked to the specific dataset version used.

D Distribution of Winning Configurations

Table 6 summarises the hyperparameter values selected by Optuna across the 55 datasets, reported as medians with ranges across outer folds. These distributions characterise the configurations that the tuning procedure converges to and may serve as informed defaults for practitioners.

Table 6: Distribution of winning configurations across 55 datasets. *Tuned hyperparameters* are selected by Optuna; *fitted properties* are emergent characteristics of the resulting model. Numeric values are median (IQR) of per-dataset fold-averaged best parameters. Categorical values show the majority choice with its frequency. Search spaces are given in table 4.

Model	Type	Parameter	Median (IQR)
ridge	HP	alpha	5.8 (1.2, 18.3)
dt	HP	max_depth	12 (10, 13)
	HP	min_samples_leaf	0.007 (0.007, 0.014)
	HP	min_samples_split	0.019 (0.014, 0.035)
	Fit	actual depth	9 (8, 11)
	Fit	leaves	72 (34, 87)
rf	HP	n_estimators	396 (285, 450)
	HP	max_depth	16 (13, 18)
	HP	max_features	0.7 (65%); 0.5 (13%); sqrt (9%)
xgb	HP	max_depth	8 (6, 9)
	HP	learning_rate	0.295 (0.292, 0.297)
	HP	subsample	0.85 (0.80, 0.90)
	HP	colsample_bytree	0.86 (0.78, 0.90)
	HP	reg_lambda	0.012 (0.005, 0.039)
	HP	min_child_weight	6.0 (3.7, 10.9)
	Fit	best iteration (early stop)	25 (17, 51)
erbf	HP	n_rbf	67 (53, 78)
	HP	n_rbf = auto	20% of datasets
	HP	alpha	0.25 (0.03, 4.4)
	HP	center_init	lipschitz (55%); kmeans (45%)
	HP	width_init	local_ridge (65%); local_variance (35%)
	Fit	effective K	60 (40, 79)
	Fit	width parameters	440 (308, 948)
chebypoly	HP	complexity	9 (4, 13)
	HP	alpha	0.69 (0.07, 2.2)
	HP	include_interactions	True: 69%; False: 31%
	HP	max_interaction_complexity	2 (median); 1 or 2
	Fit	total parameters	138 (53, 202)
chebytree	HP	complexity	2 (2, 4)
	HP	max_depth	4 (1, 9)
	HP	min_samples_leaf	0.053 (0.028, 0.066)
	HP	alpha	0.14 (0.009, 0.74)
	Fit	leaves	8 (2, 20)
	Fit	parameters per leaf	23 (14, 41)
	Fit	total parameters	198 (90, 491)

HP = tuned hyperparameter (selected by Optuna); Fit = fitted model property (emergent, not directly tuned). Categorical entries show mode with percentage; numeric entries show median (Q1, Q3) across 55 datasets.

Several patterns emerge. erbf favours Lipschitz-guided centre placement (55% of datasets) and supervised width initialisation via local ridge (65%), confirming that target-aware initialisation improves over purely geometric alternatives. Fixed centre counts are preferred (80% of datasets) with a median of 67 (IQR 53–78); the auto rule is selected for 20% of datasets (typically higher-dimensional ones), yielding a median of 60 effective centres. chebypoly converges to high polynomial degrees (median 9, IQR 4–13) with interactions enabled in 69% of datasets,

suggesting that the ridge penalty is sufficient to control the resulting high-dimensional basis. chebytree uses moderate tree depth (median 4, yielding ~ 8 leaves) with low-degree leaf polynomials (median 2), consistent with the design principle that leaf models should be simpler than a global fit to avoid overfitting small subsets. xgb selects high learning rates (median 0.295) but early stopping terminates at a median of 25 boosting rounds (IQR 17–51, out of 2000 maximum), indicating that relatively few trees suffice when the learning rate is high. rf favours large ensembles (median 396 trees) with high feature subsampling (0.7 in 65% of datasets), consistent with known good practice for random forests.

E Supplementary Results

E.1 Predictive Accuracy Rankings

Table 7: Predictive accuracy—all models (55 datasets, with tabpfn). Models ordered by mean rank on \bar{R}^2 . Top-2 = rank-1 / rank-2 counts. Best in **bold**, second underlined.

Model	Top-2	Mean Rank	Rank IQR	\bar{R}^2 median	\bar{R}^2 mean \pm std
tabpfn	44 / 5	1.49	1–1	0.872	0.798 \pm 0.201
<u>erbf</u>	<u>3 / 9</u>	<u>3.73</u>	3–5	<u>0.817</u>	<u>0.744 \pm 0.225</u>
chebytree	2 / 8	3.82	3–4	0.831	0.734 \pm 0.231
xgb	1 / <u>16</u>	3.98	2–5	0.828	0.737 \pm 0.223
chebypoly	<u>3 / 7</u>	4.45	3–6	0.791	0.709 \pm 0.229
rf	2 / 5	4.84	4–6	0.771	0.722 \pm 0.218
dt	0 / 2	6.65	6–8	0.718	0.669 \pm 0.241
ridge	0 / 2	7.04	7–8	0.597	0.576 \pm 0.231

Table 8: Predictive accuracy—CPU-viable models (55 datasets, without tabpfn). Models ranked by mean rank on \bar{R}^2 . Top-2 = rank-1 / rank-2 counts. Best in **bold**, second underlined.

Model	Top-2	Mean Rank	Rank IQR	\bar{R}^2 median	\bar{R}^2 mean \pm std
erbf	12 / <u>15</u>	2.84	2–4	0.817	0.744 \pm 0.225
<u>chebytree</u>	8 / 13	<u>2.93</u>	2–4	<u>0.831</u>	<u>0.734 \pm 0.231</u>
xgb	17 / 8	3.02	1–4	0.828	0.737 \pm 0.223
chebypoly	10 / 5	3.55	2–5	0.791	0.709 \pm 0.229
rf	7 / 6	3.89	3–5	0.771	0.722 \pm 0.218
dt	0 / 4	5.71	5–7	0.718	0.669 \pm 0.241
ridge	1 / 4	6.07	6–7	0.597	0.576 \pm 0.231

E.2 Generalisation Gap Rankings

Table 9: Generalisation gap rankings (55 datasets). Lower gap = better generalisation. Models ordered by mean gap rank. Top-2 = rank-1 / rank-2 counts. Best in **bold**, second underlined (among competitive models; ridge’s low gap reflects underfitting).

Model	Top-2	Mean Rank	Rank IQR	Gap median	Gap mean \pm std
ridge	42 / 4	1.75	1–1	0.004	0.011 \pm 0.015
chebypoly	3 / 19	3.27	2–4	0.014	0.028 \pm 0.040
<u>erbf</u>	1 / 8	<u>3.84</u>	3–5	<u>0.018</u>	<u>0.039 \pm 0.056</u>
chebytree	2 / 8	4.29	3–6	0.025	0.040 \pm 0.055
rf	2 / 7	4.98	4–6	0.024	0.061 \pm 0.096
dt	1 / 7	5.18	3–7	0.032	0.050 \pm 0.052
tabpfn	3 / 2	5.38	4–7	0.047	0.070 \pm 0.086
xgb	1 / 0	7.31	7–8	0.079	0.105 \pm 0.106

E.3 Computational Cost Details

Table 10: Computational cost (mean across 55 datasets). Tune time includes all Optuna trials for one outer fold. Predict time is per 1 000 instances. Train/1K is train time normalised per 1 000 instances, averaged across datasets; actual scaling is model-dependent. Models ordered by tune time. Fastest CPU-viable competitive model in **bold**, second underlined (tune time).

Model	Tune (s)	Train (s)	Train (ms/1K)	Predict (ms/1K)
tabpfn	0.4	4.80	871	5 131
ridge	18	0.01	3	1
dt	28	0.30	23	1
chebypoly	37	0.33	24	16
<u>chebytree</u>	<u>61</u>	0.54	82	38
xgb	203	1.10	163	17
erbf	742	16.00	1 083	11
rf	1 494	45.70	4 463	229

Each tuning trial involves inner cross-validation (3-fold for $n \geq 1000$, 5-fold otherwise), so per-trial time exceeds single-training time. Table 11 illustrates per-trial and training times on three datasets spanning the size range.

Table 11: Time per tuning trial and training time (seconds) on three datasets spanning the size range (CPU models only; tabpfn requires no per-trial tuning). Trial counts: ridge 20, dt 25, rf 25, xgb 50, erbf 30, chebypoly 30, chebytree 30.

Dataset		n	d	ridge	dt	rf	xgb	erbf	chebypoly	chebytree
concrete_strength	/trial	1 030	8	0.3	0.2	10.2	1.2	2.2	0.2	0.8
	train			0.0	0.0	6.5	0.5	1.0	0.0	0.1
california_housing	/trial	20 640	8	0.3	0.8	92.4	4.9	25.6	0.7	2.4
	train			0.0	0.4	48.3	1.2	18.1	0.2	1.1
superconduct	/trial	21 263	79	1.7	4.1	312.6	27.0	83.2	4.5	7.1
	train			0.1	2.2	217.8	8.8	51.9	2.6	3.9

F Per-Dataset Results

Table 12 presents the adjusted R^2 for each model on each of the 55 benchmark datasets. The best CPU-viable model per dataset is shown in **bold**.

Table 12: Per-dataset adjusted R^2 for all eight models, grouped by stratum. Overall best per dataset in **bold**; best CPU-viable model underlined (shown only when different from overall best). [†]Ordinal (discrete integer) target.

Dataset	tabpfn	erbf	chebytree	xgb	chebypoly	rf	dt	ridge
<i>S1: Engineering/Simulation</i>								
Ailerons	0.869	0.817	0.842	0.826	<u>0.844</u>	0.806	0.758	0.818
airfoil_noise	0.977	0.921	0.831	<u>0.923</u>	0.728	0.828	0.725	0.503
concrete_strength	0.945	0.885	0.865	<u>0.917</u>	0.892	0.880	0.809	0.597
cpu_act	0.988	0.983	0.982	0.982	<u>0.983</u>	0.976	0.968	0.736
elevators	0.929	0.862	0.886	0.873	<u>0.890</u>	0.689	0.594	0.812
energy_efficiency_heating	0.998	0.998	0.997	0.996	<u>0.997</u>	0.995	0.996	0.913
feynman_gaussian	0.999	0.969	<u>0.991</u>	0.490	0.381	0.945	0.939	0.068
feynman_wave_interference	0.999	<u>0.965</u>	0.883	0.935	0.909	0.888	0.873	0.841
friedman1	0.999	<u>0.998</u>	0.948	0.961	0.923	0.883	0.751	0.741
friedman1_d100	0.999	<u>0.998</u>	0.945	0.934	0.921	0.863	0.734	0.739
pmlb_215_2dplanes	0.948	0.948	0.948	0.947	0.948	0.947	0.948	0.705
pmlb_225_puma8NH	0.687	<u>0.686</u>	0.671	0.656	0.431	0.676	0.649	0.368
power_plant	0.967	0.948	0.944	<u>0.961</u>	0.941	0.947	0.939	0.928
<i>S2: Behavioural/Social</i>								
Bike_Sharing_Demand	0.718	0.671	0.682	<u>0.689</u>	0.644	0.668	0.654	0.333
analcata_data_supreme	0.977	0.977	0.978	0.978	0.978	0.972	0.978	0.429
food_delivery_time	—	0.252	0.335	0.346	0.331	0.284	0.278	0.181
pmlb_1028_SWD [†]	0.412	0.405	<u>0.412</u>	0.387	0.409	0.409	0.363	0.388
pmlb_1029_LEV [†]	0.544	0.548	0.538	0.501	0.551	0.524	0.478	0.551
pmlb_1030_ERA [†]	0.352	0.344	0.365	0.325	0.340	0.342	0.334	0.351
pmlb_4544_GeographicalOrigin...	0.801	0.753	0.731	0.673	<u>0.780</u>	0.702	0.515	0.779
pol [†]	0.979	0.949	0.957	<u>0.972</u>	0.869	0.950	0.926	0.465
student_performance [†]	0.269	0.200	0.221	0.255	0.228	<u>0.267</u>	0.163	0.226
wine_quality [†]	0.514	0.387	0.335	<u>0.439</u>	0.363	0.391	0.301	0.287
<i>S3: Physics/Chemistry/Life Sciences</i>								
abalone	0.586	0.556	<u>0.564</u>	0.521	0.559	0.548	0.481	0.514
diabetes	0.473	0.432	0.460	0.409	<u>0.464</u>	0.435	0.296	0.464
esol	0.916	<u>0.896</u>	0.847	0.881	0.893	0.894	0.852	0.827
freesolv	0.935	0.885	0.884	0.882	<u>0.886</u>	0.877	0.782	0.823
lipophilicity	0.592	0.387	0.329	0.390	0.331	<u>0.397</u>	0.293	0.247
particulate_matter_ukair-2017	0.744	0.740	0.746	0.741	0.750	<u>0.726</u>	0.718	0.733
physiochemical_protein	0.768	0.505	0.505	<u>0.615</u>	0.404	0.424	0.359	0.281
pmlb_503_wind	0.815	0.791	0.785	0.768	<u>0.799</u>	0.760	0.706	0.758
pmlb_522_pm10	0.398	0.398	0.094	0.296	<u>0.349</u>	0.365	0.132	0.123
pmlb_529_pollen	0.794	0.791	0.792	0.740	0.791	0.710	0.639	<u>0.792</u>
pmlb_547_no2	0.600	0.588	0.543	0.519	0.539	<u>0.599</u>	0.469	0.476
qm7	0.810	<u>0.785</u>	0.768	0.779	0.773	0.771	0.737	0.746
qsar_fish_toxicity	0.639	0.611	0.564	0.552	0.559	<u>0.615</u>	0.498	0.556
qsar_tid_11	0.649	0.528	0.519	<u>0.590</u>	0.403	0.463	0.382	0.324
sulfur	0.920	0.779	0.791	<u>0.828</u>	0.764	0.731	0.716	0.393
superconduct	0.931	0.846	0.886	<u>0.910</u>	0.819	0.856	0.821	0.675
<i>S4: Economic/Pricing</i>								
Allstate_Claims_Severity	0.539	0.496	<u>0.499</u>	0.486	0.467	0.438	0.399	0.449
Brazilian_houses	0.996	0.972	0.982	<u>0.987</u>	0.966	0.979	0.973	0.836
MiamiHousing2016	0.944	<u>0.918</u>	0.897	0.917	0.909	0.864	0.802	0.717
california_housing	0.875	0.792	0.751	<u>0.829</u>	0.730	0.739	0.667	0.601

Continued on next page

Dataset	tabPFN	erbf	chebytree	xgb	chebypoly	rf	dt	ridge
diamonds	0.947	0.945	0.943	<u>0.945</u>	0.943	0.944	0.942	0.925
fiat_500_price	0.857	0.841	0.844	0.834	0.846	<u>0.851</u>	0.823	0.840
healthcare_insurance	0.856	0.839	<u>0.856</u>	0.845	0.833	0.855	0.840	0.733
house_16H	0.583	0.491	0.502	<u>0.514</u>	0.508	0.485	0.422	0.235
house_sales	0.903	0.870	0.852	<u>0.876</u>	0.846	0.838	0.790	0.746
medical_charges	0.980	0.980	0.980	<u>0.979</u>	0.980	0.977	0.978	0.827
nyc-taxi-green-dec-2016	0.578	0.459	<u>0.530</u>	0.513	0.393	0.440	0.517	0.307
pmlb_218_house_8L	0.724	0.661	0.657	<u>0.672</u>	0.638	0.621	0.575	0.380
power_grid_stability	0.987	<u>0.951</u>	0.896	0.926	0.895	0.815	0.689	0.645
synthetic_multithreshold	0.965	0.888	0.931	0.959	0.858	0.966	0.958	0.569
synthetic_piecewise	0.963	<u>0.960</u>	0.952	0.935	0.955	0.935	0.902	0.791
synthetic_step	0.939	<u>0.877</u>	0.932	0.922	0.844	0.939	0.938	0.579

G Reproducibility and Installation

The model packages and benchmark code are publicly available under the MIT licence.

Model packages. Both packages are on PyPI and can be installed with:

```
pip install erbf poly-basis-ml
```

Source repositories:

- <https://github.com/gerberl/erbf>
- <https://github.com/gerberl/poly-basis-ml>

Benchmark code. The full benchmark—including data loaders, tuning pipeline, analysis scripts, and pre-computed results—is available at:

<https://github.com/gerberl/poly-erbf-benchmark>

To reproduce the experiments:

```
git clone https://github.com/gerberl/poly-erbf-benchmark.git
cd poly-erbf-benchmark
micromamba create -n polyerbfbench -f environment.yml
micromamba activate polyerbfbench
pip install erbf poly-basis-ml
python scripts/run_benchmark.py --max-features 50 --max-samples 50000
```

The repository README provides full instructions, including separate commands for Benchmark A (all models, preprocessed data) and Benchmark B (scalable models, full-scale data).

H Software Versions

All experiments were run under Python 3.12 using the micromamba package manager. Table 13 lists the key packages and their versions. tabPFN uses the v2.5 model weights distributed with tabPFN package version 6.3.1 and run in local GPU mode on a 24 GB TITAN RTX.

Table 13: Software versions used in all experiments.

Package	Version	Role
<i>Model implementations</i>		
tabpfn	6.3.1 (v2.5 weights)	TabPFN regressor
xgboost	3.1.3	XGBoost
scikit-learn	1.6.1	Ridge, Decision Tree, Random Forest
erbf	0.1.0	ERBF regressor
poly_basis_ml	0.2.0	ChebyPoly, ChebyTree regressors
<i>Infrastructure</i>		
Python	3.12.12	Runtime
optuna	4.6.0	Hyperparameter tuning
numpy	2.3.5	Numerical computation
scipy	1.17.0	Optimisation (L-BFGS-B for ERBF)
pandas	2.3.3	Data handling
joblib	1.5.3	Parallel execution and result serialisation
rdkit [29]	2025.09	Molecular descriptor computation
matplotlib [26]	3.10	Figure generation
seaborn [47]	0.13	Figure generation